Articles

2,3,7,8,12,13,17,18-Octafluoro-5,10,15,20-tetraarylporphyrins and Their Zinc Complexes: First Spectroscopic, Electrochemical, and Structural Characterization of a Perfluorinated Tetraarylmetalloporphyrin

Eric K. Woller and Stephen G. DiMagno*

Department of Chemistry, University of Nebraska−Lincoln, Lincoln, Nebraska 68588-0304

Received November 19, 1996[⊗]

We report a convenient and general synthesis of β-octafluoroporphyrins bearing *meso*-tetraaryl substituents, including the first synthesis and full characterization of a perfluorinated tetraarylporphyrin, perfluoro-5,10,15,20-tetraphenylporphyrin, **2**. The structural, spectroscopic, and electrochemical data indicate that β-octafluoro-*meso*-tetraarylporphyrins are a new class of *planar*, electron-deficient ligands. Particularly impressive is the 0.5 V window over which the formal oxidation potential can be tuned using only aryl substituents. The invariance of the ligand structure with increasingly positive formal oxidation potential is a key advance; electronic effects have been severed from the nonplanar conformations exhibited by all other highly electron-deficient porphyrins.

Halogenated metalloporphyrins are well-established catalysts for alkane hydroxylation and alkene epoxidation,[1−10] and β-octahalo-*meso*-tetraarylmetalloporphyrins show substantial catalytic activity and reasonable longevity in isobutane hydroxylation.[11−13] β-Octahalogenation (Cl, Br) of tetraarylporphyrins causes decreased nitrogen basicity due to σ-electron withdrawal, positive shifts in the porphyrin ring redox potentials, narrowing of the porphyrin HOMO−LUMO gap, and highly nonplanar porphyrin core structures arising from steric encumbrance at the ligand periphery.[14−17] In addition to stabilizing the porphyrin against oxidation, β-halogenation tunes the relative and absolute d-orbital energies of the ligated transition metal (and the complex's catalytic competency) through an admixture of σ, π, and steric effects.[18] While nitrogen basicity is essentially a characteristic of the σ-framework and is quite insensitive to porphyrin conformation,[19,20] the magnitude of the HOMO−LUMO gap and the redox potentials are intimately tied to the porphyrin core structure. Eduction of the relative importance of electronic and steric parameters requires electron-deficient porphyrins in which the steric and σ- and π-electronic effects are varied independently; this is currently impossible with the limited number of structurally similar ligands available.

The recent synthesis of 5,10,15,20-tetrakis(heptafluoropropyl)porphyrin (THFPP),[21−23] a ruffled porphyrin displaying an optical spectrum typical of a planar macrocycle, demonstrated that π-electronic properties in other nonplanar electron-deficient porphyrins are intertwined with substituent effects. The spectroscopic features of THFPP strongly suggest that increased conjugation of aryl groups is responsible for the bathochromic shifts and concomitant destabilization of the porphyrin HOMO observed for nonplanar β-octabromo- and β-octachlorotetraarylporphyrins.[23]

The small radius and high electronegativity of fluorine imply that β-perfluorinated metalloporphyrins should be the first examples of *planar*, highly electron-deficient porphyrins; AM1 semiempirical calculations of 2,3,7,8,12,13,17,18-octafluoro-5,10,15,20-tetraphenylporphyrin, **1(Zn)**, predict a nearly planar macrocycle with essentially orthogonal phenyl rings.[24] Such a structure

[⊗] Abstract published in *Advance ACS Abstracts*, February 15, 1997.

(1) Chang, D. K.; Ebina, F. *J. Chem. Soc., Chem. Commun.* **1981**, 778.
(2) Hoffman, P.; Robert, A.; Meunier, B. *Bull. Soc. Chim. Fr.* **1992**, *129*, 85.
(3) Traylor, P. S.; Dolphin, D.; Traylor, T. G. *J. Chem. Soc., Chem. Commun.* **1984**, 279.
(4) Traylor, T. G.; Tsuchiya, S. *Inorg. Chem.* **1987**, *26*, 1338.
(5) Traylor, T. G.; Hill, K. W.; Fann, W.-P.; Tsuchiya, S.; Dunlap, B. E. *J. Am. Chem. Soc.* **1992**, *114*, 1308.
(6) Gonsalves, A. M. d. A. R.; Johnstone, R. W. W.; Pereira, M. M.; Shaw, J.; Sobral, A. J. F. d. N. *Tetrahedron Lett.* **1991**, *32*, 1355.
(7) Mansuy, D. *Coord. Chem. Rev.* **1993**, *125*, 129.
(8) Meunier, B. *Chem. Rev.* **1992**, *92*, 1411.
(9) Fujii, H. *J. Am. Chem. Soc.* **1993**, *115*, 4641.
(10) Wijesekera, T. P.; Lyons, J. E.; Ellis, P. E., Jr. *Catal. Lett.* **1996**, *36*, 69.
(11) Ellis, P. E., Jr.; Lyons, J. W. *Coord. Chem. Rev.* **1990**, *105*, 181.
(12) Ellis, P. E., Jr.; Lyons, J. E. *Catal. Lett.* **1989**, *3*, 389.
(13) Grinstaff, M. W.; Hill, M. G.; Labinger, J. A.; Gray, H. B. *Science* **1994**, *264*, 1311.
(14) Ochsenbein, P.; Ayougou, K.; Mandon, D.; Fischer, J.; Weiss, R.; Austin, R. N.; Jayaraj, K.; Gold, A.; Terner, J.; Fajer, J. *Angew. Chem., Int. Ed. Engl.* **1994**, *33*, 348.
(15) Bhyrappa, P.; Krishnan, V. *Inorg. Chem.* **1991**, *30*, 239.
(16) Wijeskera, T.; Matsumoto, A.; Dolphin, D.; Lexa, D. *Angew. Chem., Int. Ed. Engl.* **1990**, *29*, 1028.
(17) Birnbaum, E. R.; Schaefer, W. P.; Labinger, J. A.; Bercaw, J. E.; Gray, H. B. *Inorg. Chem.* **1995**, *34*, 1751.
(18) Grinstaff, M. W.; Hill, M. F.; Birnbaum, E. R.; Schaefer, W. P.; Labinger, J. A.; Gray, H. B. *Inorg. Chem.* **1995**, *34*, 4896.
(19) Gassman, P. G.; Ghosh, A.; Almlof, J. *J. Am. Chem. Soc.* **1992**, *114*, 9990.
(20) Ghosh, A. *J. Am. Chem. Soc.* **1995**, *117*, 4691.
(21) DiMagno, S. G.; Williams, R. A.; Therien, M. J. *J. Org. Chem.* **1994**, *59*, 6943.
(22) Goll, J. G., Moore, K. T., Ghosh, A.; Therien, M. J. *J. Am. Chem. Soc.* **1996**, *118*, 8344.
(23) DiMagno, S. G.; Wertsching, A. K.; Ross, C. R., II. *J. Am. Chem. Soc.* **1995**, *117*, 8279.
(24) Results from the AM1 semiempirical calculations (Dewar, M. J. S.; Zoebisch, E. G.; Healy, E. F.; Stewart, J. J. P. *J. Am. Chem. Soc.* **1985**, *107*, 3902) are included in the Supporting Information. These calculations predict a planar macrocycle for **1(Zn)**. The free base is predicted to have a shallow potential energy surface on which the planar structure is a local minimum approximately 3 kcal/mol above the global minimum.

S0022-3263(96)02159-7 CCC: $14.00

Table 1. Spectroscopy of Free Base Porphyrins

compd[a]	Soret band[b] λ_{max} (nm)	Q bands λ_{max} (nm)	B(0,0)−Q(0,0) splitting[c] (cm^{-1})	NH Shift[d] (ppm)	ref
1	402	499, 532, 581, 637	7630	−4.18	this work
2	392	493, 579, 632	8210	−4.23	this work
3	406	500, 533, 581, 636	7390	−4.14	this work
P	394	489, 519, 561, 613	7590	−3.93	this work
OMP[e]	377	494, 530, 564, 618	9000	−3.76	38
TPP	418	514, 549, 590, 646	7080	−2.79	this work
TPFPP	412	506, 584, 638	7300[f]	−2.91	30
THFPP	404.5	510, 545, 594, 647	7820	−2.30	22
OCTPFPP	436	536, 622	7070[f]	−1.0	30
OBTPFPP	454	552, 636	6610[f]	−0.5	30

[a] Abbreviations: P, porphine; OMP, 2,3,7,8,12,13,17,18-octamethoxyporphyrin; TPP, 5,10,15,20-tetraphenylporphyrin; TPFPP, 5,10,15,20-tetrakis(perfluorophenyl)porphyrin; THFPP, 5,10,15,20-tetrakis(heptafluoropropyl)porphyrin; OCTPFPP, 2,3,7,8,12,13,17,18-octachloro-5,10,15,20-tetrakis(perfluorophenyl)porphyrin; OBTPFPP, 2,3,7,8,12,13,17,18-octabromo-5,10,15,20-tetrakis(perfluorophenyl)porphyrin. [b] Absorption spectra of the free bases were recorded in CH_2Cl_2 unless otherwise noted. [c] Calculated from $B(0,0) - [(Q_x(0,0) + Q_y(0,0))/2]$. [d] NMR spectra were recorded in $CDCl_3$. [e] The optical spectrum was recorded in toluene. [f] The energies of the unreported Q bands were estimated using a vibrational spacing of 1500 cm^{-1}.

is consistent with an optical spectrum hypsochromically shifted in comparison to TPP. In stark contrast to this prediction, a putative synthesis of 2,3,7,8,12,13,17,18-octafluoro-5,10,15,20-tetrakis(pentafluorophenyl)porphyrin, **2**, by direct fluorination produced a compound possessing a distinctly red-shifted absorption spectrum (Soret band at 430 nm) characteristic of a highly nonplanar macrocycle.[25] Several reports of metalated perfluorinated porphyrins appear in the patent literature; however, no characterization data for these compounds have been published.[26]

Herein, we report a convenient and general synthesis of β-octafluoroporphyrins bearing *meso* tetraaryl substituents, including the synthesis, characterization, and X-ray structure determination of a perfluorinated metalloporphyrin, **2(Zn)**. The spectroscopic data for the newly synthesized compounds indicate that the previous report was erroneous and that the structures of β-octafluoroporphyrins are correctly predicted by semiempirical molecular orbital theory.

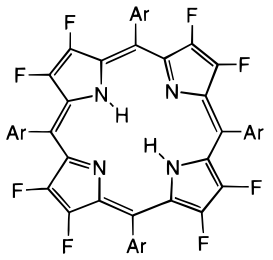

1. Ar = Phenyl
2. Ar = Pentafluorophenyl
3. Ar = 3-Methoxyphenyl

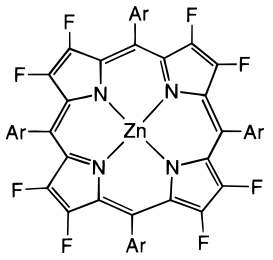

1(Zn). Ar = Phenyl
2(Zn). Ar = Pentafluorophenyl

Results and Discussion

Octafluoroporphyrins were prepared by the acid-catalyzed condensation of 3,4-difluoropyrrole[27] and the corresponding benzaldehyde, followed by oxidation. The synthetic procedures generally followed those outlined by Lindsey,[28] except that a greater than stoichiometric amount of BF_3 etherate "catalyst" was employed and the reactions were quenched with DDQ after only 0.5−1 h. The yields of porphyrins were similar to those obtained when unsubstituted pyrrole was condensed with the same aldehydes; 33%, 21%, and 20% for **1**, **2**, and **3**, respectively.[29] The preparation of **1** could also be scaled up (10 mmol each of pyrrole and benzaldehyde, 500 mL CH_2Cl_2) with no loss in yield. The use of trifluoroacetic acid as the catalyst resulted in precipitously reduced yields of porphyrin and slower reaction rates. Sparingly soluble **1** was isolated by recrystallization from toluene/pentane, while chromatographic workup was performed for the fairly soluble compounds **2** and **3**. Interestingly, the perfluorinated derivative, **2**, demonstrated enhanced volatility in comparison to TPP or **1**, commensurate with the reduced London dispersion forces characteristic of perfluorocarbons. Sublimation of **2** to yield thin films could be performed under moderate vacuum.

Compound **3** was synthesized to examine the extent of atropisomerism and the rate of aryl rotation in octafluorotetraarylporphyrins. Three isomers of **3** with identical optical spectra were chromatographically separated. No interconversion was observed, signaling very slow aryl rotation in these compounds. This steric effect mirrors that in metalated tetrakis(perfluorophenyl)porphyrin, a compound in which slow aryl rotation has been demonstrated.[30] Surprisingly, one isomer of **3** accounted for more than 95% of the isolated product. Coordination of the methoxy groups to the excess BF_3 etherate at the porphyrinogen stage may be the basis for this unusual selectivity.

Deprotonation of **1** and **2** with an excess of the hindered, non-nucleophilic base 1,8-diazabicyclo[5.4.0]-undec-7-ene (DBU) yields bluish-green monoanions. Spectrophotometric determinations in CH_2Cl_2 show that the NH in **1** is less acidic than the protonated DBU by 3.9 pK_a units. In contrast, no deprotonation of TPP was observed with DBU up to the highest base concentration examined, 0.3 M; thus, **1** is *at least* 1000 times more acidic than TPP in CH_2Cl_2. The dramatic σ-electron-withdrawing effect of pentafluorophenyl substituents is evident in the pK_a of **2**. The porphyrin NH is *more* acidic than protonated DBU by 0.2 pK_a units; even treatment of **2** with triethylamine results in a visible color change.

^{1}H NMR spectroscopy of the free bases reveals that the NH resonances of **1**−**3** are shifted upfield in comparison to other benchmark porphyrins (Table 1). This chemical

(25) Tsuchiya, S.; Seno, M. *Chem. Lett.* **1989**, 263.
(26) Lyons, J. E., Ellis, P. E., Jr. U.S. Patent 5,120,886, 1992. Ellis, P. E., Jr.; Lyons, J. E. U.S. Patent 4,970,348, 1990.
(27) Leroy, J.; Wakselman, C. *Tetrahedron Lett.* **1992**, *35*, 8605.
(28) Lindsey, J. S.; Schrieman, I. C.; Hsu, H. C.; Kearney, P. C.; Marguerettaz, A. M. *J. Org. Chem.* **1987**, *52*, 827.
(29) Typical isolated yields for TPP and TPFTPP are 36% and 15%, respectively, in our hands.
(30) Birnbaum, E. R.; Hodge, J. A.; Grinstaff, M. W.; Schaefer, W. P.; Henling, L.; Labinger, J. A.; Gray, H. B. *Inorg. Chem.* **1995**, *34*, 3625.

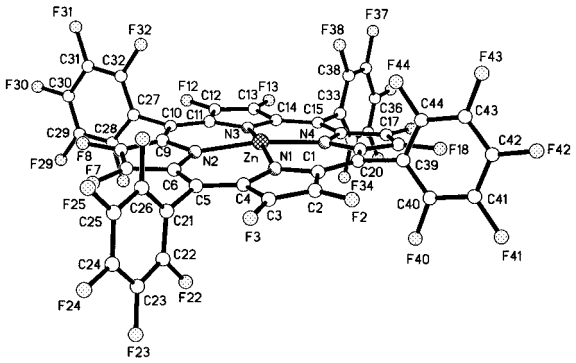

Figure 1. Perspective drawing of **2(Zn)** showing numbering scheme. The axial ligand in the five-coordinate structure has been removed for clarity.

shift is typical of highly symmetrical, planar porphyrins without conjugating *meso* substituents, indicating a solution structure in which the aryl groups are essentially orthogonal. Also evident from Table 1 is that nonplanar distortions decrease the ring current; this effect is amplified in β-octahalogenated (Cl and Br) tetraarylporphyrins because increased conjugation of the phenyl groups with the central ring is possible in the twisted conformation, thereby making the porphyrin π-orbitals more diffuse.

Variable-temperature ^{19}F spectroscopy in $CDCl_3$ shows two well-resolved porphyrin signals at low temperature (−50 °C, 470 MHz) for **1**−**3**. These signals coalesce at approximately 40 °C; thus, the NH proton exchange is occurring in each case with an approximate $\Delta G^{\ddagger} = 13$ kcal/mol. Proton transfer is a degenerate process in symmetrical porphyrins; thus, the rate should be halved in order to obtain the true barrier height for the process.[31] However, we have reported the observed (raw) free energy of activation to simplify direct comparison with the earlier literature. The larger free energy of activation compared to the analogous process in TPP[32] is consonant with decreased basicity of the nitrogen sp^2 orbitals and a contraction of the NH bond in this innersphere proton transfer. (Expansion of the porphyrin core is also a plausible explanation for the higher activation barrier.) Variable-temperature ^{1}H (500 MHz) and ^{19}F (470 MHz) spectroscopy of **3** revealed no additional exchange processes over the temperature range −50 to 50 °C.

The absorption spectra of **1**−**3** show large hypsochromic shifts in comparison to other tetraarylporphyrins, particularly in the Soret (B) band region of the spectra (Table 1). Also cataloged in the table are B(0,0)−Q(0,0) energy differences for selected porphyrins. The B and Q bands arise from the electron interaction between two pairs of nearly degenerate lowest excited singlets: the *x*-polarized $^1(b_1 \rightarrow c_2)$ and $^1(b_2 \rightarrow c_1)$ states and the *y*-polarized $^1(b_1 \rightarrow c_1)$ and $^1(b_2 \rightarrow c_2)$ states.[33,34] Two factors determine the extent of the electron interaction and, thus, the magnitude of the B(0,0)−Q(0,0) splitting: the degeneracy of the states[35,36] and the compactness of the orbitals involved.[37] If the frontier orbitals are delocalized onto peripheral substituents, the overall electron interaction is smaller. Compounds **1** and **3** possess extremely large B(0,0)−Q(0,0) energy differences for *meso*-tetrasubstituted porphyrins, rivaled only by a comparable separation in *meso*-(perfluoroalkyl)porphyrins. The energy difference in **2** is the largest ever reported for a *meso* tetrasubstituted porphyrin and is surpassed only by the extremely hypsochromically shifted β-octaalkoxyporphyrins.[38,39] Consistent with the ^{1}H NMR data, the aryl groups in **1**−**3** are predicted to be nearly orthogonal in this analysis because delocalization of electron density onto the *meso*-substituents would decrease the B(0,0)−Q(0,0) separation. The absorption spectrum of **2** also shows vanishingly small $Q_x(0,0)$ and $Q_y(0,0)$ bands, characteristic of a free base porphyrin with energetically degenerate HOMOs.[36]

Table 2. Average Bond Lengths (Å) and Bond Angles (deg) for 2(Zn) and Selected Metalloporphyrins

parameter	ref core of least strain	**2(Zn)**	Zn(TPP)(THF)$_2$	Zn(TPyP)(py)	Zn(TPP)
N−C$_t$	2.010	2.051	2.057	2.047	2.036
N−Zn	2.010	2.059	2.057	2.073	2.036
N−C$_a$	1.384	1.382	1.371	1.369	1.375
C$_a$−C$_b$	1.446	1.439	1.444	1.447	1.443
C$_b$−C$_b$	1.355	1.337	1.349	1.355	1.351
C$_a$−C$_m$	1.395	1.397	1.403	1.406	1.399
C$_a$−N−C$_a$	105.4	107.4	107.0	106.6	106.5
N−C$_a$−C$_b$	110.3	108.3	109.3	109.8	109.6
N−C$_a$−C$_m$	125.4	125.5	125.8	125.7	125.7
C$_a$−C$_b$−C$_b$	107.0	108.0	107.2	106.9	107.2
C$_a$−C$_m$−C$_a$	124.6	126.0	125.0	125.2	125.0
ref	41	this work	42	43	44

A perspective drawing from the X-ray crystal structure determination of **2(Zn)** is shown in Figure 1.[40] Average bond lengths and angles for **2(Zn)** and selected porphyrins are given in Table 2.[41−44] The zinc complex is five coordinate with split occupancy (acetonitrile (70%) or THF (30%)) of the axial site in the crystal examined. Mixed solvation appears to be a common, albeit curious, structural motif for zinc porphyrins bearing pentafluorophenyl groups.[45] The four nitrogen atoms form a plane (0.006 Å average deviation) from which the zinc atom is displaced 0.173 Å toward the pendant axial ligand. This displacement is somewhat smaller than is typical for five-coordinate zinc porphyrins. The zinc−nitrogen bond lengths average 2.059 Å and are within the reported range (2.052−2.076 Å).[42] Thus, **2(Zn)** possesses a modestly expanded porphyrin core (2.052 Å N-Ct distance) for a five coordinate zinc complex, but it is smaller than that observed for six coordinate TPP(Zn)·(THF)$_2$.[42] The core expansion results from widening of the C$_a$−C$_N$−C$_b$,

(31) Crossley, M. J.; Field, L. D.; Harding, M. M.; Sternhell, S. *J. Am. Chem. Soc.* **1987**, *109*, 2335.

(32) Eaton, S. S.; Eaton, G. R. *J. Am. Chem. Soc.* **1977**, *99*, 1601. Values for proton tautomerism in tetraaryl porphyrins are in the range 11.9−12.5 kcal/mol.

(33) Gouterman, M. *J. Mol. Spectrosc.* **1961**, *6*, 138.

(34) Gouterman, M. In *The Porphyrins*; Dolphin, D., Ed.; Academic Press: New York, 1978; Vol. III, p 1.

(35) Binstead, R. A.; Crossley, M. J.; Hush, N. S. *Inorg. Chem.* **1991**, *30*, 1259.

(36) Spellane, P. J.; Gouterman, M.; Antipas, A.; Kim, S.; Liu, Y. C. *Inorg. Chem.* **1980**, *19*, 386.

(37) The interaction between any two excited singlet configurations, $\langle {}^1\chi_{ik}|H|{}^1\chi_{jl}\rangle = 2\langle\Psi_j\Psi_k|g|\Psi_l\Psi_i\rangle - \langle\Psi_j\Psi_k|g|\Psi_i\Psi_l\rangle$, depends upon the interelectronic distances ($g = 1/r$). Mataga, N.; Kubota, T. *Molecular Interactions and Electronic Spectra*; Marcel Dekker: New York, 1970.

(38) Merz, A.; Schropp, R.; Lex, J. *Angew. Chem., Int. Ed. Engl.* **1993**, *32*, 291.

(39) Merz, A.; Schropp, R.; Dötterl, E. *Synthesis* **1995**, 795.

(40) The atomic coordinates for this structure have been deposited with the Cambridge Crystallographic Data Centre. The coordinates can be obtained, on request, from the Director, Cambridge Crystallographic Data Centre, 12 Union Road, Cambridge, CB2 1EZ, UK.

(41) Hoard, J. L. *Ann. N. Y. Acad. Sci.* **1973**, *206*, 18.

(42) Schauer, C. K.; Anderson, O. P.; Eaton, S. R.; Eaton, G. R. *Inorg. Chem.* **1985**, *24*, 4082.

(43) Collins, D. M.; Hoard, J. L. *J. Am. Chem. Soc.* **1970**, *92*, 3761.

(44) Scheidt, W. R.; Kastner, M. E.; Hatano, K. *Inorg. Chem.* **1978**, *17*, 706.

(45) Marsh, R. E.; Schaefer, W. P.; Hodge, J. A.; Hughes, M. E.; Gray, H. B. *Acta Crystallogr.* **1993**, *C49*, 1339.

Table 3. Spectroscopic and Electrochemical Data[a] for Zinc Porphyrins in CH_2Cl_2

compd[b]	B and Q bands λ_{max} (nm)	B(0,0)−Q(0,0) splitting[c] (cm^{-1})	$E^{+2/+1}$	$E^{+1/0}$	$E^{0/-1}$	$E^{-1/-2}$
1(Zn)	406, 502, 536, 573	7180	1.36	1.26	−1.03	*d*
2(Zn)	407, 496, 537, 568(s)	6960	*d*	1.70[e]	−0.63	−1.04
TPP(Zn)[f,g]	419, 548, 586	6800	1.16	0.80	−1.33	−1.66
TPFPP(Zn)[g]	412, 543, 578	6970	1.58	1.37	−0.95	−1.37
OCTPFPP(Zn)[g]	442, 576	6560	1.57	1.63	−0.47	−0.75
OBTPFPP(Zn)[g]	455, 585	6180	1.53	1.57	−0.48	−0.76

[a] Cyclic voltammetry conditions: porphyrin concentration, 1 mmol; sweep rate, 50 mV/s; 0.1 M $TBAPF_6$; fc/fc^+ internal standard (0.48 V); Ag/AgCl reference. [b] Abbreviations are the same as in Table 1. [c] Calculated from B(0,0)−Q(0,0). Unreported Q(0,0) bands were estimated by assuming a vibrational spacing of 1300 cm^{-1}. [d] Irreversible process. [e] Oxidation of the porphyrin occurs at the limit of the solvent. [f] Our measurements are in accord with the literature data (ref 52). [g] Data from the last four table entries are from ref 52.

$C_a-C_m-C_a$, and $C_b-C_a-C_m$ bond angles and compression of the $N-C_a-C_b$ bond angle, in accord with the general trends delineated by Hoard.[41] Although the bond angles vary in a typical manner for radially expanded metalloporphyrins, the alterations in pyrrole bond lengths are reversed. Whereas the C_b-C_b bond is normally observed to lengthen as result of radial core expansion, for **2(Zn)** the bond length is quite short. Similarly, the C_a-C_b bond is compressed in **2(Zn)** while the $N-C_a$ bond length resembles that of Hoard's reference porphyrin of least strain.[41] The strong σ-electron-withdrawing effect of fluorine is responsible for the localized contraction of the C_b-C_b and C_a-C_b bonds, while lone pair donation into the delocalized porphyrin π^* orbitals partially compensates for this effect. Thus, bond lengths approach the normal values distant from the site of fluorine substitution.

The porphyrin ring is slightly ruffled with the major deviations from the porphyrin mean plane occurring at the *meso*-positions; these displacements are −0.174 Å (C5), 0.148 Å (C10), −0.110 Å (C15), and 0.203 Å (C20) for the indicated atoms. Given that crystal packing forces are sufficient to cause this degree of nonplanar distortion for even sterically unencumbered porphyrins,[46,47] the origins of the ruffling cannot be determined with certainty. The slight ruffling in the structure of **2(Zn)** contrasts strongly in type and magnitude with the drastic nonplanar *saddle* distortions observed for metal complexes of β-octabrominated (OBTPFP) and β-octachlorinated (OCTPFP) analogs.[30,45,48−50] Due to the short C−F bond lengths, porphyrin ring fluorine atoms would be collinear with the first carbon atoms in the aryl groups if **2(Zn)** were planar. For example, in Figure 1 a line drawn between F2 and F18 would intercept C39. A pure S_4 saddle distortion of the macrocycle cannot alleviate this unfavorable collinear arrangement at the porphyrin periphery; such a conformational change can only increase the distance along the F−C−F line of sight. In contrast, the slight vertical displacement of the phenyl group in the ruffled conformation obviates this steric interaction while causing a minimal nonplanar distortion of the macrocycle.

The pentafluorophenyl groups in **2(Zn)** are at an average dihedral angle of 83° to the mean porphyrin plane. The probable origin for the near perpendicularity of the aryl substituents lies in the close contacts between the β-fluorine substituents and the aryl ring carbon atoms. These contacts average 2.77 Å and fall within a narrow range; the minimum distance is 2.742 Å for C27−F12, and the maximum distance is 2.785 Å for C39−F2. The sum of the van der Waals radii is (1.47 Å for fluorine and 1.77 Å for aromatic carbon)[51] is 3.24 Å. A search of the data base from the Cambridge Crystallographic Data Centre revealed more than 100 structures with C−F nonbonded distances less than 2.8 Å; thus, the contact distances in this case are short but not exceptional. Finally, it should be noted that the orthogonality of the aryl rings in the solid-state structure is consistent with the solution-phase spectroscopic measurements.

The electrochemical and optical properties of the zinc complexes and reference compounds are summarized in Table 3.[52] The metalated porphyrins exhibit many of the same optical features found for the free base: a blue shift in the Soret absorption compared to TPP(Zn), a large splitting between the B(0,0)−Q(0,0) band, and a small molar extinction coefficient for Q(0,0). Metalation raises the a_{2u} orbital energy, lifting the near degeneracy of the HOMOs observed for free base. The Q(0,0) band is clearly observable in the zinc complexes **1(Zn)** and **2(Zn)**, but the Q(0,0)/Q(1,0) ratio remains small.[36] The optical absorption data strongly suggest that no gross change in macrocycle structure occurs upon metalation.

The redox potentials of **1(Zn)** and **2(Zn)** were measured by square wave and cyclic voltammetry in CH_2Cl_2. β-Octafluorination of TPP results in 480 and 300 mV positive shifts in the formal potentials of the first oxidation (+1.26) and first reduction (−1.03), respectively, while perfluorination results in 900 and 700 mV positive shifts. From the standpoint of porphyrin ring oxidation, **2(Zn)** is the most electron-deficient zinc porphyrin ever reported. The onset of irreversible oxidation of **2(Zn)** occurs at the solvent breakdown of CH_2Cl_2, so the apparent potential (+1.70 V) must be regarded as approximate. In view of the positive shift in the formal potential for the first reduction (−0.63) and the blue shift in the Q(0,0) optical absorption of **2(Zn)** compared to **1(Zn)**, the reported value for the ring oxidation should be quite close to the actual formal potential. Finally, the electron-withdrawing effects of β- and *meso*-substituents are nearly additive for **2(Zn)**, in contrast to other β-octahalogenated porphyrins. The constancy of substituent effects is consistent with planar solution structures for both **1(Zn)** and **2(Zn)**.

Conclusion

The structural, spectroscopic, and electrochemical data indicate that β-octafluoro-*meso*-tetraarylporphyrins are

(46) Scheidt, W. R.; Lee, Y. J. *Struct. Bonding* **1987**, *64*, 1.
(47) Ravikanth, M.; Chandrashekar, T. K. *Struct. Bonding* **1995**, *82*, 105.
(48) Mandon, D.; Ochsenbein, P.; Fischer, J.; Weiss, R.; Jayaraj, K.; Austin, R. N.; Gold, A.; White, P. S.; Brigaud, O.; Battioni, P.; Mansuy, D. *Inorg. Chem.* **1992**, *31*, 2044.
(49) Henling, L. M.; Schaefer, W. P.; Hodge, J. A.; Hughes, M. E.; Gray, H. B. *Acta Crystallogr.* **1993**, *C49*, 1743.
(50) Schaefer, W. P.; Hodge, J. A.; Hughes, M. E.; Gray, H. B. *Acta Crystallogr.* **1993**, *C49*, 1342.
(51) Bondi, A. *J. Phys. Chem.* **1964**, *68*, 441.
(52) Hodge, J. A.; Hill, M. G.; Gray, H. B. *Inorg. Chem.* **1995**, *34*, 809.

a new class of *nearly planar*, electron-deficient ligands. Particularly impressive is the 0.5 V window over which the formal oxidation potential can be tuned using only substituents on *orthogonal* aryl rings. The invariance of the ligand structure with increasingly positive formal oxidation potential is a key advance; electronic effects have been severed from the nonplanar conformations exhibited by all other highly electron-deficient porphyrins. Future studies of structure−function relationships in metalloporphyrin-catalyzed reactions will benefit from the extended range of accessible ligand formal potential and nitrogen basicity offered by β-octafluorinated porphyrins.

Experimental Section

Instrumentation and Materials. Manipulations of air- and water-sensitive reagents were carried out either in a glovebox (Innovative Technologies Labmaster 150) or by standard Schlenk techniques. THF was distilled from sodium/benzophenone prior to use. Methylene chloride was distilled from CaH_2. Benzaldehyde and BF_3 etherate were distilled immediately prior to use. The remaining reagents were obtained from Aldrich or Fisher Chemical Cos. and used as received. Optical spectra were performed using an OLIS-14 modification of a Carey-14 UV−vis−NIR spectrometer. NMR spectra were obtained in the instrumentation center at the University of Nebraska using 300, 360, or 500 MHz spectrometers. Proton NMR spectra were collected in $CDCl_3$ using the residual protiochloroform as a chemical shift reference (7.24 ppm). ^{19}F NMR was conducted at 470 MHz. Chemical shifts are given with reference to an added internal standard, $CFCl_3$. Analyses were conducted by Desert Analytics, Tucson, AZ.

2,3,7,8,12,13,17,18-Octafluoro-5,10,15,20-tetraphenylporphyrin (1). Benzaldehyde (0.35 mL, 3.5 mmol), 3,4-difluoropyrrole (0.33g, 3.2 mmol), and 250 mL of distilled CH_2Cl_2 were placed under N_2 in a 500 mL round-bottom flask equipped with a magnetic stir bar. The reaction was stirred while BF_3 etherate (0.5 mL, 3.9 mmol) was added via syringe. To monitor the reaction, aliquots were periodically removed from the reaction vessel, oxidized with DDQ, neutralized with pyridine, and chromatographed by silica gel TLC using $CHCl_3$ as eluent. After 30 min, DDQ (1 g) and pyridine (5 mL) were added. The reaction was stirred for 12 h, filtered through a short silica gel column using CH_2Cl_2 as eluent, and evaporated. The resulting solid was washed three times with 10 mL of pentane followed by three washes with 10 mL of ethanol. The product was recrystallized from toluene/hexane by layering to yield 127 mg of pure **1** in 21% yield (first crop). A second crystallization using identical conditions yielded an additional 75 mg for a total isolated yield of 33%: ^1H NMR (360 MHz, $CDCl_3$) δ 8.03 (d, 8 H, $J_1 = 6.7$ Hz), 7.74 (m, 12 H), −4.18 (s, 2 H); ^{19}F NMR (500 MHz, $CDCl_3$, −50 °C) δ −141.1 (s, 4 F), −146.4 (s, 4 F); UV−vis (CH_2Cl_2) 402 (5.31), 499 (4.21), 532 (3.71), 581 (3.55), 637 (3.60); low resolution FAB MS 758 (calcd 758). Anal. Calcd for $C_{44}H_{22}F_8N_4$: C, 69.66; H, 2.92; N, 7.38. Found: C, 69.43; H, 2.90; N, 6.95.

2,3,7,8,12,13,17,18-Octafluoro-5,10,15,20-tetrakis(pentafluorophenyl)porphyrin (2). Pentafluorobenzaldehyde (0.3 mL, 2.4 mmol), 3,4-difluoropyrrole (226 mg, 2.2 mmol), and 250 mL of dry CH_2Cl_2 were placed under N_2 in a 500 mL round-bottom flask equipped with a magnetic stir bar. The reaction was stirred while the BF_3 etherate (1 mL, 7.8 mmol) was added via syringe. To monitor the reaction, aliquots were periodically removed from the reaction vessel, oxidized with DDQ, neutralized with pyridine, and chromatographed by silica gel TLC using $CHCl_3$ as eluent. After 30 min, DDQ (0.5 g) and pyridine (3 mL) were added. The reaction was stirred for 12 h and filtered through a short silica gel column using CH_2Cl_2 as eluent, and the solvent was evaporated. The product was purified by silica gel chromatography with pentane. Collection was continued until the eluent was colorless. The solvent was removed, and the resulting product was recrystallized from $CHCl_3$ to yield reddish purple crystals that lost solvent upon standing. This material was dried under vacuum to yield 129 mg of pure **2**: ^1H NMR (360 MHz, $CDCl_3$) δ −4.22 (s, 2 H); ^{19}F δ (500 MHz, $CDCl_3$, $CFCl_3$ internal standard, −50 °C) −161.0 (t, 8 F, $J = 20.9$ Hz), −149.6 (t, 4 F, $J = 20.8$ Hz), −147.9 (s, 4 F), −142.9 (s, 4 F), −138 (d, 8 F, $J = 17.8$ Hz); UV−vis (CH_2Cl_2) 392 (5.24), 493 (4.29), 579 (3.71); low-resolution FAB MS 1118 (calcd 1118). Anal. Calcd for $C_{44}H_2F_{28}N_4$: C, 47.25; H, 0.18; N, 5.01. Found: C, 47.25; H, 0.05; N, 4.86.

2,3,7,8,12,13,17,18-Octafluoro-5,10,15,20-tetrakis(3-methoxyphenyl)porphyrin (3). *m*-Anisaldehyde (0.3 mL, 2.5 mmol), 3,4-difluoropyrrole (215 mg, 2.1 mmol), and 100 mL of dry CH_2Cl_2 were placed under N_2 in a 250 mL round-bottom flask equipped with a magnetic stir bar. The reaction was stirred while BF_3 etherate (0.9 mL, 7.1 mmol) was added via syringe. To monitor the reaction, aliquots were periodically removed from the reaction vessel, oxidized with DDQ, neutralized with pyridine, and chromatographed by silica gel TLC using $CHCl_3$ as eluent. After 30 min, DDQ (1 g) and pyridine (3 mL) were added. The reaction was stirred for 12 h and filtered through a short silica gel column using CH_2Cl_2 as eluent, and the solvent was evaporated. A rough purification was done using a silica gel column with $CHCl_3$ as eluent. The solvent was removed, and the product was further purified on silica gel using chloroform/hexane (1:4). The pure fractions were combined and concentrated to afford 88.8 mg of pure **3** in 20% yield: ^1H NMR (360 MHz, $CDCl_3$) δ 7.65 (t, 12 H), 7.30 (m, 4 H), 4.02 (s, 12 H), −4.14 (s, 2 H); ^{19}F δ (500 MHz, $CDCl_3$, −50 °C) δ −140.9 (s, 4 F), −146.0 (s, 4 F); UV−vis (CH_2Cl_2) 406 (5.31), 500 (4.22), 533 (3.67), 581 (3.57), 636 (3.56); low-resolution FAB MS 878 (calcd 878). Anal. Calcd for $C_{48}H_{30}F_8N_4O_4$: C, 65.61; H, 3.44; N, 6.38. Found: C, 64.49; H, 3.46; N, 5.61.

General Metalation Procedure for β-Octafluorinated Porphyrins. The porphyrin (50 mg) was suspended in 20 mL of 1:1 CH_2Cl_2:THF solution containing a 10-fold excess of $ZnCl_2$. Several drops of triethylamine were added to the solution; metalation commenced immediately and was complete within 5 min. The mixture was partitioned between CH_2Cl_2 and water and extracted. The organic layer was washed, dried over $MgSO_4$, filtered through a short silica gel column, and evaporated. **1(Zn)** and **2(Zn)** were crystallized from hot acetonitrile.

[2,3,7,8,12,13,17,18-Octafluoro-5,10,15,20-tetraphenylporphinato]zinc, 1(Zn): ^1H NMR (500 MHz, $CDCl_3$) δ 7.99 (dd, 8 H, $J_1 = 6.8$ Hz, $J_2 = 1.6$ Hz), 7.75 (tt, 4 H, $J_1 = 7.6$ Hz, $J_2 = 1.2$ Hz), 7.69 (t, 8 H, $J_1 = 7.6$ Hz); ^{19}F NMR (500 MHz, $CDCl_3$) δ −143.3 (s); UV−vis (CH_2Cl_2) 406 (5.60), 502 (3.49), 536 (4.31) 573 (3.62); FAB MS 820 (calcd 820).

[2,3,7,8,12,13,17,18-Octafluoro-5,10,15,20-tetrakis(pentafluorophenyl)porphinato]zinc, 2(Zn). The crystalline compound isolated from the above procedure contained 0.5 equiv of THF and 0.5 equiv of acetonitrile: ^{19}F NMR (500 MHz, $CDCl_3$) δ −139.6 (dd, 8 F, $J_1 = 23.4$ Hz, $J_2 = 7.4$ Hz), −145.4 (s, 8 F), −150.7 (t, 4 F, $J_1 = 19.8$ Hz), −161.9 (td, 8 F, $J_1 = 23.4$ Hz, $J_2 = 8.6$ Hz); UV−vis (CH_2Cl_2) 407 (5.45), 537 (4.30); FAB MS 1180 (calcd 1180).

Structure Determination of 2(Zn). The selected crystal of **2(Zn)** $[N_4C_{44}F_{28}]Zn[CH_3CN)_{0.69}/(THF)_{0.31}]$ was, at 20 ± 1 °C, monoclinic, space group $P2_1/n$ (an alternate setting of $P2_1/c - C^5_{2h}$ (No. 14)) with $a = 16.168(4)$ Å, $b = 16.856(4)$ Å, $c = 18.301(4)$ Å, $\beta = 91.65(2)°$, $V = 4985(2)$ Å^3, and $Z = 4$ [$d_{calcd} = 1.642$ g/cm^3, μ_a(Mo Kα) = 0.64 mm^{-1}]. A total of 8216 independent absorption-corrected reflections having 2θ(Cu Kα) < 48.3° (the equivalent of 0.70 limiting Cu Kα spheres) were collected on a computer-controlled Nicolet autodiffractometer using ω scans and graphite-monochromated Mo Kα radiation. The structure was solved using "heavy-atom" Patterson techniques with the Siemens SHELXTL-PC software package as modified at Crystalytics Co. The resulting structural parameters have been refined to convergence [R_1 (unweighted, based on F) = 0.055 for 3638 independent absorption-corrected reflections having 2θ(Mo Kα) < 48.3° and $I > 3\sigma(I)$] using counter-weighted full-matrix least-squares techniques and a structural model that incorporated anisotropic thermal parameters for all nonhy-

drogen atoms except disordered carbon atoms C_{1s} and C_{3s}, which were included in with isotropic thermal parameters.

The fifth coordination site of the Zn atom is occupied by the nitrogen of an acetonitrile ligand 69% of the time and the oxygen of a THF ligand 31% of the time. C_{1s}, C_{3s}, and $C4_{3s}$ were included in the structural model as carbon atoms with occupancy factors of 0.31 and carbon atom C_{5s} with an occupancy factor of 0.69. The position occupied by carbon atom C_{2s} is a methylene carbon 31% of the time and a methyl carbon 69% of the time. The geometry for partial occupancy THF ligand coordinated to the Zn atom was restrained in the least-squares refinement cycles. The C−C bond length between methylene carbons was included in the least-squares refinement as a free variable that refined to a final value of 1.49(2) Å, and the $C_{1s}-C_{3s}$ and $C_{2s}-C_{4s}$ separations were restrained to be 1.633 times this value. The lattice also contains disorder solvent molecules between solvent molecules between porphyrin molecules near the crystallographic inversion at the origin of the unit cell. Carbon atom C_{6s} was included in the structural model with an occupancy of 0.75.

Acknowledgment. We thank Professor Victor Day of this department for performing the crystal structure analysis of **2(Zn)** and Crystalytics Company of Lincoln, Nebraska for the use of its equipment and supplies for this structure analysis. We thank Professors Jody Redepenning and Richard Shoemaker for their assistance and helpful discussions. This work was supported by the Centers for Materials Research and Metallobiochemistry at the University of Nebraska, and NSF/EPSCoR.

Supporting Information Available: A summary of the semiempirical AM1 calculations for **1** and **1(Zn)**; optical spectra of **1**, **2**, **1(Zn)**, and **2(Zn)**; spectrophotometric pK_a determination for **2**; variable-temperature ^{19}F NMR spectra for **2**; and representative mass spectra (18 pages). This material is contained in libraries on microfiche, immediately follows this article in the microfilm version of the journal, and can be ordered from the ACS; see any current masthead page for ordering information.

JO962159T